A MODEL FOR THE MECHANICAL INTERACTION BETWEEN SOLID BREEDER AND CLADDING MATERIALS

GEORGE E. ORIENT, NASR M. GHONIEM
Mechanical Aerospace and Nuclear
Engineering Department
University of California Los Angeles
Los Angeles, California 90024
(213) 825-4866

ABSTRACT

Mechanical interaction between the solid breeder material and its cladding during power cycles is an important consideration in the design of solid breeder blankets. The analysis presented in the paper gives a design tool for material choices and lifetime prediction for breeder pins. The UCLA solid breeder blanket design is evaluated, and operating conditions are suggested. The material model for the pellet includes linear thermoelastic behavior and swelling. The cladding is assumed to be thin and to exhibit swelling and creep. Two alternate breeder/cladding material pairs have been analyzed, a Li_2O/2.25Cr-1Mo and a $LiAlO_2$/9-C design. While high swelling excludes the Li_2O/2.25Cr-1Mo design, it is found that in the $LiAlO_2$/9-C case compatibility of thermal expansion between the breeder and the cladding as well as low swelling of the breeder result in less than 0.5% total plastic strain after one year of operation.

I. INTRODUCTION

The use of solid breeders in blanket components of fusion reactors is governed by the need for tritium breeding, with avoidance of problems arising from liquid metal breeders, such as corrosion and MHD pressure drops. However, solid breeders have a relatively low fracture strength and poor mechanical properties. Their ability to withstand mechanical loads and thermal gradients is greatly reduced, leading to intolerable design limits. Another problem with solid breeder materials is the high retention of tritium and helium if the breeder is fully dense. To allow for tritium diffusion, and as a practical solution to their mechanical problems, solid breeders can be produced as porous square cylinders of dimensions on the order of 1-3 cm. Such cylinders, called pellets, are encapsuled in a structural cladding material that provides for a barrier to their interaction with the coolant. Moreover, the cladding material carries existing structural and thermal loads. The UCLA solid breeder pin-type blanket is described in detail in reference 1. and will be used in the present analysis. The first wall is cooled with high velocity helium through coolant channels, while the pins are cooled by helium in a cross-flow configuration. The first zone is made up entirely of beryllium pins for neutron multiplying, and then two solid breeder zones follow.

In order to minimize maintenance time, a satisfactory configuration has to withstand transient phenomena associated with power-ramps and shutdowns while giving optimal thermo-mechanical performance with a reasonable lifetime. These objectives can be reached by selecting suitable geometry and material specifications as well as prescribed temperature histories. Finding the minimal allowable ramp rate for startup is important for the economy of operation, since overly conservative startup can lead to a reduction in the net energy output. The main concern in a preliminary design is failure of the cladding due to high stresses or large total strains. The following analysis provides a simplified tool for design based on macroscopic mechanical interaction between the breeder and the cladding. The next most important effect to include in the analysis is phenomena associated with failure of materials at the microscopic level such as stress corrosion, creep fracture and fatigue. Some of these aspects of pellet-cladding interaction are covered in reference 2.

II. THEORETICAL FORMULATION

A. Assumptions and Model Restrictions

Since the thermal field exhibits only a slight azimuthal asymmetry[1], the problem is formulated based on an axisymmetric analytical solution for the radial temperature distribution. Interaction between the changing geometry and the thermal field has been neglected during the course of the analysis.

The ends of the rods are assumed to be unconstrained, which results in zero net force. Consequently, plane stress formulation is used throughout the analysis. Also, the deformations are assumed to be small. The thickness of the cladding is assumed to be small compared to its diameter, which leads to thin shell formulation in the cladding.

Material models for the pellet include linear elastic behavior, linear thermal expansion and temperature dependent swelling. The cladding material is assumed to exhibit linear elastic behavior, linear thermal expansion and temperature dependent creep. All linear material properties are taken as constants.

A quasi-static solution method is employed, since the frequency of changes in the thermal field are small as compared to the structure's eigenfrequencies. The presence of material and geometrical imperfections is also neglected in the present analysis.

The time dependent temperature field is also represented in a quasi-static manner as follows:

$$T(r,t) = T_{preheat} + (R(r) - T_{preheat})\, T(t),$$

where R(r) is the steady state temperature profile and T(t) is a dimensionless shape function corresponding to the power cycles.

For this analysis, densification of the pellet material is neglected due to lack of available data. This material nonlinearity might also be an important component in the interaction, but is not treated here. Its effect is expected to lower the contact stresses. The current analysis provides a conservative estimate of cladding behavior.

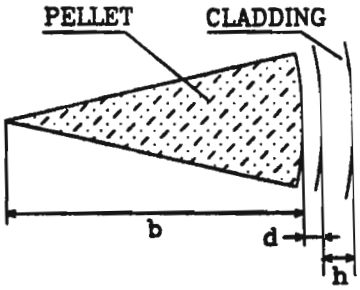

Fig. 1. Geometry, notations

B. General Solution for the Pellet

With the notations shown on Fig 1. the strain-displacement relations corresponding to the above specified assumptions are as follows:

$$\epsilon_t = \frac{u}{r} \tag{1}$$

$$\epsilon_r = \frac{du}{dr} \tag{2}$$

The strain-stress relations give:

$$\epsilon_r = \frac{1}{E}\left[(1+\nu)\sigma_r - \nu\sigma_{kk}\right] + \alpha T + \epsilon^{sw}/3 \tag{3}$$

$$\epsilon_t = \frac{1}{E}\left[(1+\nu)\sigma_t - \nu\sigma_{kk}\right] + \alpha T + \epsilon^{sw}/3 \tag{4}$$

$$\sigma_{kk} = \sigma_{rr} + \sigma_{tt} \tag{5}$$

where r and t subscripts denote radial and tangential quantities, respectively, ϵ^{sw} is the swelling strain, and the temperature is measured from some base value, T_o. The 1/3 factor gives dilatational strains from the volumetric strain when infinitesimal strains are assumed.

Equilibrium equations for an axisymmetric stress state reduce to one single equation:

$$\frac{d\sigma_r}{dr} + \frac{\sigma_r - \sigma_t}{r} = 0. \tag{6}$$

Substituting the strain-displacement relations into the constitutive equations, then the stresses into the equilibrium equation, we arrive at the displacement form of equilibrium.

$$\frac{d}{dr}\left[\frac{1}{r}\frac{d(ru)}{dr}\right] = \frac{1+\nu}{1-\nu}\frac{d}{dr}(T\alpha + \epsilon^{sw}/3) \tag{7}$$

The solution of this equation for an axisymmetric solid cylinder is:

$$u_r = \frac{(1+\nu)}{r}\int_a^r [\alpha T(r',t)+\epsilon^{sw}(r',t)/3]r'dr' + Cr$$

$$= \Theta(r,t) + Cr \tag{8}$$

$$\sigma_r = \frac{E}{r^2}\int_a^r [\alpha T(r',t)+\epsilon^{sw}(r',t)/3]r'dr' +$$

$$C\frac{E}{1-\nu} = \Phi(r,t) + CA \tag{9}$$

$$\sigma_t = \Phi(r,t) - E[\alpha T(r,t) + \epsilon^{sw}/3] + CA \tag{10}$$

Equation (8) represents the radial displacement of the pellet at any given position r while equations (9) and (10) give the two dimensional stress field within the cross-section of the pellet. The auxiliary functions Θ and Φ defined in (8) and (9) are introduced for compactness.

C. General Solution for the Cladding

The strain-displacement relation is given by:

$$2\epsilon = \frac{2u}{b+d} \tag{11}$$

Also, the stress-strain relation is:

$$2\sigma_t = 2E[2\epsilon - 2\alpha\, 2T(t) - c\epsilon - \epsilon^r] \tag{12}$$

where the notation is as follows:

$^2\epsilon$: total strain in the cladding
$^c\epsilon$: accumulated creep strain
ϵ^r : residual strain present, zero at initial state, and superscript 2 denotes quantities associated with the cladding, in general.

D. Boundary Conditions

Continuity of displacements and traction:

$$u_r(b,t) - d = {}^2u(t) \tag{13}$$

$$-[p_0 + \sigma_r(b,t)]\,\frac{b+d}{h} = {}^2\sigma_t \tag{14}$$

where p_0 denotes the coolant pressure which produces compressive stress in the cladding. Since the radial stress in the pellet is negative, equation (14) gives the right signs after contact. Equations (13) and (14) lead to the following integral equation for the unknown function C(t):

$$C(t) = F(t)+\epsilon^c\left(-\frac{b+d}{h}\,[\Phi(b,t)+AC(t)],T(b+d,t),t\right) \tag{16}$$

where

$$\delta = \frac{b+d}{h}\,A + {}^2E\,\frac{b}{b+d}$$

$$F(t) = \frac{1}{\delta}\left[-\frac{b+d}{h}\,(\Phi(b,t)+p_0) - \frac{\Phi(b,t)-d}{b+d} + {}^2E({}^2\alpha T(t) + \epsilon^r + \epsilon^{sw}/3)\right] \tag{17}$$

and $\epsilon^c\,(\sigma(t),T(t),t)$, denotes the functional that gives the total creep strain due to a load history $\sigma(t)$ and temperature history T(t). Assuming time-hardening (which is identical to strain-hardening for continuous loads), the creep strain functional has the following form:

$$\epsilon^c = \int_0^t \left[\frac{\delta\hat{e}(\xi,\eta,t')}{\delta t'} + \frac{\delta\hat{e}(\xi,\eta,t')}{\delta\eta}\,\frac{\delta\eta}{\delta t'}\right]_{\substack{\xi=\sigma(t')\\ \eta=T(t')}} dt' \tag{18}$$

where $\hat{e}(\sigma,T,t)$ is the uniaxial creep response of the material to constant load σ and temperature T and is given in reference 3. Equation (16) is in the form of the familiar nonlinear Volterra equation of the second kind. The numerical solution is based on the implicit trapezoidal rule discussed in some detail in reference 4. The order of the method is two, which means that the global error behaves like $O(h^2)$. The present system shows stiffness in the solution, since after initial transients die out, the solution exhibits a slowly varying, quasi-steady state behavior. Accurate representation of this initial transient is important, because it also contributes to the total accumulated strains present at the beginning of the subsequent cycle. This, in turn, defines the behavior during the next transient.

E. Effect of the power cycles

To simulate real operational conditions, a typical time history shown in Fig. 2 is used. One cycle consists of a power ramp, operation at full power, shutdown and dwell time at preheat temperature. If creep deformation occurs during the cycle, there will be residual plastic strain in the cladding after it separates from the pellet. This effect is equivalent to a permanent increase in the diameter of the cladding and causes it to reach contact in the subsequent startup at a later time within the cycle. Since the formulation given above is valid only during contact, the residual strains accumulated during contact and the total time spent under swelling conditions have to be followed carefully in the course of the numerical solution.

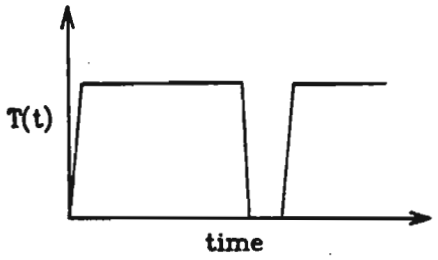

Fig. 2. Time history T(t) for assumed cyclic loading

III. MATERIAL CHOICES AND PROPERTIES

Two sets of materials are considered in this analysis. We will first analyze the combination of a Li_2O solid breeder clad with 2.25Cr-1-Mo steel. Then we present the same analysis for $LiAlO_2$ and the 9-C martensitic steel. The corresponding material properties are given in reference 3. The most important differences between the material pairs are: compatibility of thermal expansion between $LiAlO_2$ and 9-C, and the swelling of Li_2O is higher than that of $LiAlO_2$.

IV. RESULTS

Although superposition of the phenomena driving the pellet-cladding interaction is not possible due to their nonlinearity, their effects can be studied qualitatively in separate analyses. In order to obtain quantitative data, an integrated analysis accounting for all the process included in the model has to be performed. In the following, we present results of calculations illustrating the effects of various important variables on the pellet-cladding mechanical interaction problem.

A. Effect of Solid Breeder/Cladding Compatibility

In Fig. 3 and 4 the stresses for different

designs under the same thermal operating conditions are shown. The curves correspond to startup scenarios leading to full operation after 0.5, 2 and 5 days, respectively. The blanket is preheated at 550 °C. The preheat time does not affect the results for this analysis, since the initial contact stresses are always smaller than the threshold stress for creep. If no creep occurred, the elastic stress levels would be around 800 MPa for both cases at operating temperature.

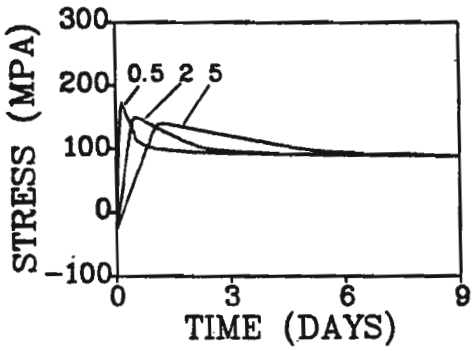

Fig. 3. $LiAlO_2$/9-C design, no gap

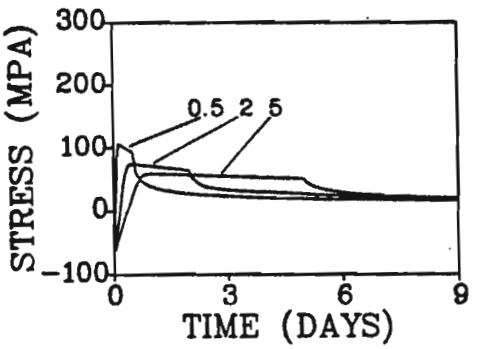

Fig. 4. Li_2O/2.25Cr-1-Mo design, 0.15 mm gap

A discontinuity occurs in the stress rates when the temperatures attain the full operation values. The reason for this is twofold: the time derivative of the cladding temperature is zero, consequently, the second term in (18) vanishes. On the other hand, the forcing function given in (17) becomes constant. The discontinuity is more pronounced in the Li_2O/2.25Cr-1-Mo case. Swelling of the pellet has been neglected for these runs. Since the coefficients of thermal expansion for the $LiAlO_2$/9-C design are closer, the difference in the displacement of the pellet surface and the cladding is smaller. Consequently, the same elastic stress levels occur at significantly smaller gap sizes, which is advantageous both for thermohydraulics and operation purposes. In fact, for the $LiAlO_2$/9-C design zero initial gap is safe, as will be shown in the integrated analysis.

B. Effect of initial gap thickness

Fig. 5 shows the stress histories in the cladding due to a ramp variation of the center temperature for Li_2O/2.25Cr-1-Mo materials. Contact occurs at a later time for larger initial gap thickness. Consequently, the resulting thermal stresses are much lower. A 0.03 mm reduction in the gap size results in contact at the preheating temperature, which is indicated by initial high tensile stresses. This effect seems to drive the whole interaction for a given set of materials. One implication is that tolerances are expected to play a crucial role in operation when the breeder and cladding materials are incompatible thermomechanically.

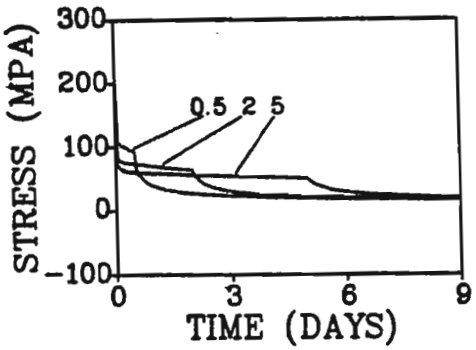

Fig. 5. Li_2O/2.25Cr-1-Mo design, 0.12 mm gap

C. Effect of preheating

Preheating is the third most important effect in the interaction process. Fig. 6 shows the results for the same material choice, steady state temperature profile and geometry as those for Fig. 3. This time the system is not preheated to 550 °C.

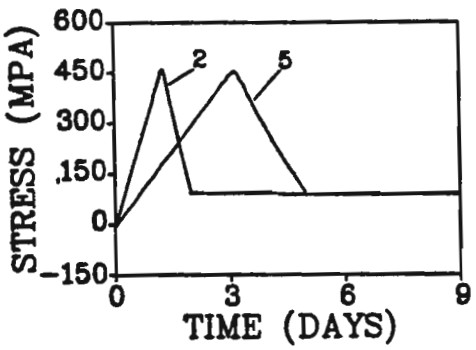

Fig. 6. $LiAlO_2$/9-C design, no gap

Since the coefficient of the thermal expansion for the cladding is slightly higher than that for the pellet, initially there is no contact when the pin is preheated. Compressive stress due to

the coolant pressure develops in the cladding. The stress value is about one third of the critical buckling stress, which represents an adequate margin of safety. The advantage of preheating from a structural point of view is that interaction occurs at high temperature, allowing for creep relaxation. Therefore stress relaxation can act during startup to relieve the peak stress. At different characteristic locations of the blanket similar stress histories prevail, and the first row of the second Li zone shows the highest peak stress. Further cyclic calculations were performed for this particular location.

D. Effect of the temperature ramp

When the slope of the temperature ramp is low, the cladding can creep more before a steady state profile is attained and the resulting displacement helps to accommodate the thermal expansion of the pellet. However, for practical startup scenarios this mechanism is found to have small impact on the results.

E. Effect of pellet swelling: integrated analysis

Fig. 7 illustrates the interaction under cyclic operation when swelling of the pellet is included for the same geometry and material selection as the previous figure.

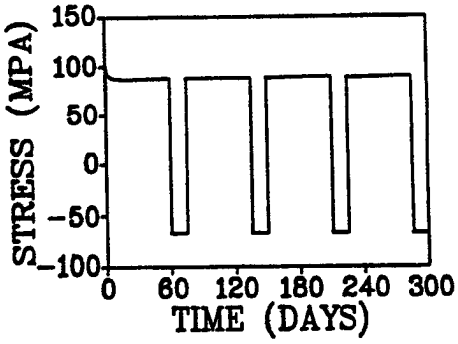

Fig. 7. $LiAlO_2$/9-C design, no gap

As a result of residual strains accumulated in the first cycle, contact in the second cycle occurs at a later time. Therefore, the stress level is lower as compared to the first cycle. For the particular geometry shown here, the stress barely exceeds the value of the "back-stress" defining a threshold for creep. Consequently, creep strain is very low. If swelling did not expand the pellet, stresses would asymptotically tend to the "back-stress". This threshold value at the cladding temperature is 87 MPa for 9-C and 18 MPa for 2.25Cr-1-Mo.[3] Swelling gradually builds up, and instead of the decreasing stresses, we see a slight increase and eventually higher stress levels. The actual increase (about 5 MPa) is rather small in one year. Another quantity limiting the lifetime of the pin is the accumulated plastic strain. Fig. 8 depicts the plastic strain and the elastic strain over four cycles for the $LiAlO_2$/9-C design.

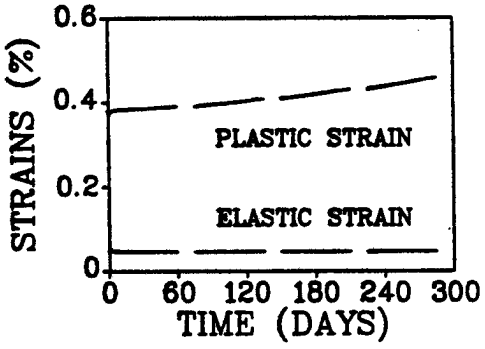

Fig. 8. $LiAlO_2$/9-C design, no gap

The elastic strains decrease with time, which reflects the stress relaxation process. On the other hand, plastic strains increase with time. The plastic strains stay below 0.5%, and the elastic strain accumulated after the first startup is less than 0.05%. Extrapolating this value for the expected life of three years, the design is safe based on the 1% accumulated plastic strain criterion. In Fig. 9 the same stress and strain components can be seen for the Li_2O/2.25Cr-1Mo design over one period.

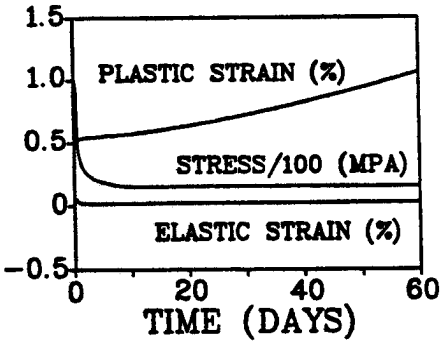

Fig. 9. Li_2O/2.25Cr-1-Mo design, 0.15 mm gap

In this case swelling of the pellet is stronger, but the creep rate is also higher, therefore stresses remain low. On the other hand, the accumulated plastic strain exceeds the 1% value by the end of the first power-cycle, which indicates failure.

V. CONCLUSIONS

The analysis presented here can be used as a design tool to define allowable startup scenarios

and substantiate material selection based on mechanical constraints. For the analyzed blanket preheating at 550 °C is necessary and the $LiAlO_2$/9-C design is more attractive. Better compatibility of thermal expansion results in safe stress levels even at zero gap thickness. This is particularly important, since sensitivity of the interaction to the gap size would impose stringent requirements on manufacturing of the parts. More importantly, however, high plastic deformation of the cladding due to strong swelling of LI_2O yields short lifetime of the Li_2O/2.25Cr-1-Mo design. Densification of the breeder material would alleviate this problem, but the stresses within the breeder are very low due to the thin cladding geometry. Consequently, densification is expected to be insignificant.

ACKNOWLEDGEMENT

This work was supported by the U. S. Department of Energy, Office of Fusion Energy, Grant #DE-FG03-80ER52061, with UCLA.

References:

[1] S. GROTZ, and N. M. GHONIEM, "Thermal Analysis of a Pin-Type Blanket for Tokamak Reactors" In the Proceedings of this meeting, also UCLA-ENG-8612/PPG-938 (1986).
[2] J. YU-CHEN YAUNG, "A Model of Pellet Cladding Interaction to Simulate Operational Ramp Failure of Water Reactor Fuel" Ph.D. Thesis UCLA (1983).
[3] S. SHARAFAT, R. AMODEO, and N. M. GHONIEM "Materials Data Base and Design Equations for the UCLA Solid Breeder Blanket" UCLA-ENG-8611/PPG-937 (1986).
[4] C. W. GEAR, Numerical Initial Value Problems in Ordinary Differential Equations, Prentice-Hall, Englewood Cliffs (1971).